ISSN 0021-3640, JETP Letters, 2024, Vol. 119, No. 7, pp. 556–563. © The Author(s), 2024. This article is an open access publication.
Russian Text © The Author(s), 2024, published in Pis'ma v Zhurnal Eksperimental'noi i Teoreticheskoi Fiziki, 2024, Vol. 119, No. 7, pp. 552–559.

BIOPHYSICS

Analysis of Skin Neoplasms' Raman Spectra Using the Lorentz Approximation Method: Pilot Studies

I. N. Saraeva[a,*], E. N. Rimskaya[a], A. B. Timurzieva[a,b], A. V. Gorevoy[a], S. N. Sheligyna[a], V. I. Popadyuk[c], E. V. Perevedentseva[a], and S. I. Kudryashov[a]

[a] *Lebedev Physical Institute, Russian Academy of Sciences, Moscow, 119991 Russia*
[b] *N.A. Semashko National Research Institute of Public Health, Moscow, 105064 Russia*
[c] *Peoples' Friendship University of Russia named after Patrice Lumumba, Moscow, 117198 Russia*
**e-mail: saraevain@lebedev.ru*

Received December 22, 2023; revised March 7, 2024; accepted March 7, 2024

Confocal Raman microspectroscopy provides the ability to diagnose cancer by quantitatively analyzing spectral features and identifying underlying biochemical changes. The differentiation of malignant skin neoplasms (basal cell carcinoma, squamous cell carcinoma), benign skin neoplasms (papilloma) and healthy skin was carried out by obtaining Raman spectra in vitro with excitation wavelengths of 532 and 785 nm. We present a new method for analyzing the parameters of spectral bands, based on the calculation of the second derivative and Lorentz approximation of the spectra. Using this method on a small selection of skin tumors, we have demonstrated that processes in skin tumors can cause deformation of the proteins' secondary structure, leading to degradation and shift of the corresponding bands (972, 1655 cm^{-1}) to the lower frequency. Bands corresponding to lipids in skin neoplasms either broaden and increase or split into two peaks (bands 1061, 1127, 1297, 1439, 1745 cm^{-1}). The disruption of lipid structure, also indicated in several bands as a shift to lower wavenumbers, is possibly due to increased cell membrane fluidity in tumors. The results of the study may be useful for the development of optical biopsy methods for early diagnosis of tumors.

DOI: 10.1134/S0021364023604153

1. INTRODUCTION

The differentiation of benign and malignant skin tumors has been studied for several years both in vitro and in vivo [1–7]. Cancer causes changes in the structure of tissue cells that can be detected using microspectroscopy. The most commonly used spectral post-analysis methods include standard principal component analysis (PCA) [8, 9], multivariate curve resolution analysis (MCR) [3, 5], partial least squares discriminant analysis (PLS/DA) [8–13] and others that allow the detection of basal cell carcinoma (BCC) and squamous cell carcinoma (SCC). Processes in tumors lead to an increase in the nuclear-cytoplasmic ratio (the ratio of the area of the nucleus and the cytoplasm), disruption of the chromatin structure, and changes in the content of lipids and proteins [14]. Using confocal Raman microspectroscopy, the authors of one of the studies [15] demonstrated that the contribution of nucleic acids, histones and proteins to the Raman spectra of tumor cell nuclei differs from that in normal epidermal cells. It has been established that the dermis near the tumor borders is deficient in collagen and has signs of structural changes.

In this work, we propose a differentiation method based on the analysis of the second derivative of Raman spectra obtained upon excitation at wavelengths of 532 and 785 nm [9, 16, 17]. The search for hidden peaks by calculating the second derivative is widely used in the analysis of infrared (IR)-Fourier transmission/reflection spectra, for example, to study processes occurring under the influence of certain antibacterial agents [18, 19]. However, it is used less frequently in Raman spectroscopy [20–26], and for the analysis of skin tumors—for the first time in our article.

Analysis of the second derivative of Raman spectra makes it possible to detect differences in the parameters of spectral bands, such as wavenumber, FWHM of the band, and area, which contain important information about the conformational order/disorder of the corresponding molecular bond and help to understand the fundamental changes that occur during tumor formation. Thus, the broadening of amide bands is often associated with the resulting disruption of the secondary structure of proteins, which can be caused by cell damage or mutation. This kind of analysis of spectral bands is most effectively carried out using the Lorentz approximation of spectra, where the difference between control (healthy skin) and pathol-

ogy is more clearly visible in the spectra of the second derivative.

In this work, we provide a comparative analysis of BCC, PCC, papilloma and normal skin by calculating the second derivative spectra and determining the peak parameters (spectral position, bandwidth, area under the curve).

2. EXPERIMANTAL DETAILS

Samples of healthy skin and tumors were obtained by surgical removal. A preliminary diagnosis was made by a dermatologist-oncologist, and an accurate diagnosis after removal of the tumor was obtained using histological studies (the "gold standard" of diagnosis). Each tumor along with intact tissue was placed in saline. Raman spectra were recorded for seven samples of BCC, five SCC, three papillomas and five healthy skin samples, from 10 to 20 spectra at different points in each sample. A total of 21 samples of skin tumors from male and female patients, aged from 37 to 73 years, were studied. The samples corresponded to diagnosed cases of papilloma, carcinoma, skin cancer and healthy skin. All samples were stored under the same conditions (0.9% NaCl solution). More detailed information is given in Table S1 in the supplementary materials.

Raman spectra were obtained using a Renishaw inVia Basis spectrometer (inVia InSpect, Renishaw, London, UK) with excitation at 785 nm, energy up to 45 mW, acquisition time 10 s using a 50× objective (NPlan 50/0.50 Leica, Wetzlar, Germany), as well as Confotec MR520 spectrometer (SOL Instruments, Minsk, Belarus) at a laser wavelength of 532 nm, laser power 15 mW, accumulation time 2 s, using a 40× objective (MPlanFL, Nikon, Tokyo, Japan) with a numerical aperture of 0.75 and a working distance of 0.66 mm.

Background fluorescence signal was removed from the recorded spectra using the Vancouver algorithm, which is an improved multi-polymodal baseline removal method optimized for fluorescence of biomedical samples (degree 5 polynomial was used) [27]. The resulting spectra were smoothed and normalized to the most intense Raman bands in the range 1200–1800 cm^{-1} [16].

The averaged processed spectra for each sample were approximated using the Lorentzian fit using OriginPro software (OriginPro 2019b 9.6.5.169) according to the established method [18, 19]. The fitting procedure consists in approximating the shape of the peaks in the processed Raman spectra to the shape of the Lorentz contour:

$$y = y0 + \frac{2A}{\pi}\frac{w}{4(x - x_c)^2 + w^2}, \quad (1)$$

where $H = 2A/(\pi w)$ is the peak height, A is the area under the curve, w is the bandwidth (FWHM), x_c is the maximum position (central wavenumber in inverse centimeters), y_c and y_0 are the maximal and background signals, correspondingly (Fig. 1).

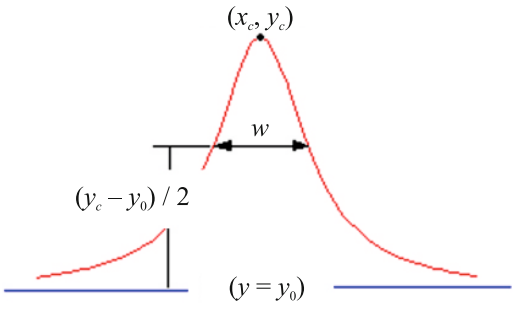

Fig. 1. (Color online) Schematic representation of the Lorentz contour, according to which the Raman spectra are approximated.

Detection of Raman bands (hidden peaks) was carried out by determining local maxima of the second derivative with Savitsky–Golay smoothing. The found values (positions of the maxima of the second derivative) were fixed, after which all peaks were approximated by the Lorentzian fit (1), as a result of which the values of the bandwidth and area under the curve were obtained. The distribution of these values (standard deviation) was estimated by the program in accordance with the noise level estimate and the magnitude of the residual error.

3. RESULTS AND DISCUSSION

3.1. Second Derivatives of Raman Spectra

Averaged Raman spectra for normal skin, BCC, SCC, and papillomas obtained upon excitation at wavelengths of 532 and 785 nm (hereinafter mentioned in the text as λ_{532} and λ_{785}), and their second derivatives are presented in Fig. 2.

The parameters of the spectral bands were obtained by the Lorentz approximation method described in Section 2. These values are displayed in Tables S2, S3, where each cell includes up to three rows corresponding to the position of the maximum, the bandwidth (FWHM) and the area under the curves with standard errors (Table S2, interpretation of spectral bands is given according to data from [9, 28–35]; Table S1 in supplementary materials).

3.1.1. DNA/RNA. The band at 1085 cm^{-1}, assigned to PO_2 vibrations in nucleic acids [28, 34, 35], shifts towards higher wavenumbers in the spectra of BCC and papilloma at λ_{785}, and for all tumors—to lower wavenumbers at λ_{532} (Fig. 2 and Table S2). At λ_{532} the area under the curve decreases significantly in the spectra of SCC, and the bandwidth increases in the spectra of neoplasms, decreasing for all tumors at λ_{785}.

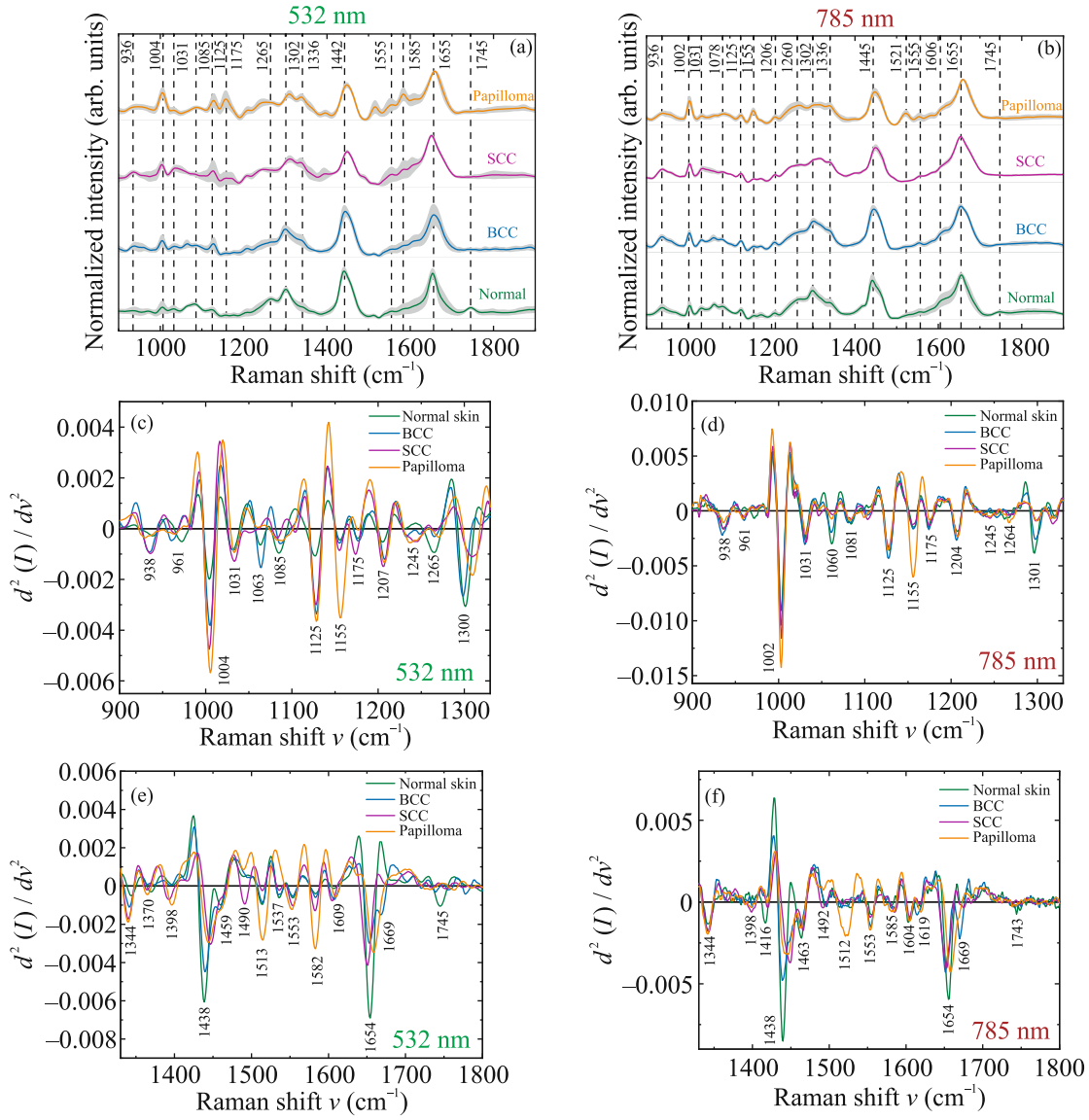

Fig. 2. (Color online) Averaged Raman spectra of healthy skin (normal skin, green line) and neoplasms (basal cell carcinoma (BCC), blue line); squamous cell carcinoma (SCC), purple line; papilloma (orange line), obtained at two excitation wavelengths: 532 nm (a) and 785 nm (b). The gray penumbra indicates the standard deviation. The corresponding spectra of the second derivative, obtained at two excitation wavelengths: 532 nm (c, e) and 785 nm (d, f), are presented in two regions: (c, d) from 900 to 1330 cm^{-1} and (e, f) from 1330 to 1800 cm^{-1}.

A drop in intensity and a shift towards lower wavenumbers has been reported previously [36], and such deviation can be caused by single- and double-strand DNA breaks [37]. Another PO_2-related band appears in all spectra of tumors at both laser excitation wavelengths in the range ~1100–1104 cm^{-1} [38]. This band results from excessive DNA replication during tumor growth [31]. Band at 1175 cm^{-1}, related to cytosine (C) and guanine (G) [39], shifts towards higher wavenumbers for BCC and papilloma and vice versa for SCC (Fig. 2 and Table S3). For λ_{785} it shifts to higher wavenumbers in all tumor spectra.

The area for the DNA/RNA band centered at 1344 cm^{-1} [40] increases in the spectra of SCC and papilloma at both excitation wavelengths (Fig. 2 and Table S2). The broadening of the bands at λ_{785} may result from the destruction of nucleic acids [28, 31, 37]. In the spectra of papilloma, the band area increases significantly, which can be explained by more intensive DNA replication in malignant neoplasms [28, 37].

Ring symmetric (breathing) modes in adenine (A), G are displayed in the spectra as a band at 1490 cm^{-1} [41–43]. This band was detected only in the spectra of

SCC and papilloma at λ_{532} and in all samples except papilloma at λ_{785} (Fig. 1, Table S2).

3.1.2. Cell membrane damage. The band centered at 1031 cm^{-1}, corresponding to molecular vibrations of phospholipids, narrows in SCC and broadens in papilloma at both excitation wavelengths; its intensity increases in the spectra of papilloma at λ_{532} (Fig. 2 and Table S2) and in the spectra of SCC at λ_{785}. Stretching vibrations of the C-C chain of cell wall lipids lead to the appearance of a peak at 1063 cm^{-1} [28, 44], which broadens in the BCC spectra and its area increases. The peak is absent in SCC and papilloma. At λ_{785} the peak increases, and its area grows in all tumor's spectra. The 1127 cm^{-1} band, which can be attributed to lipids, in the spectra of neoplasms narrows at λ_{532}, although the corresponding area increases. At λ_{785} there is no significant change in bandwidth or area.

3.1.3. Lipids. The band at 1301 cm^{-1}, attributed to CH_2 in saturated lipids, is sensitive to disruption of conformational order in cells [28–30, 45]. Its position shifts towards higher frequencies in the spectra of SCC and papilloma at λ_{532} and in all tumors' spectra—at λ_{785} (Fig. 2, Table S2). The band broadens in BCC and SCC, its area increases at both laser excitation wavelengths. A shift towards higher wavenumbers indicates deformation of the molecular structure of lipids (higher content of gauche conformers) [28, 39, 45]. The band at 1398 cm^{-1}, attributed to CH_3 oscillations, in the spectra of skin tumors shifts towards lower wave numbers (Fig. 2, Table S2), and its intensity increases significantly in spectra of SCC and papilloma (Figs. 2a, 2b) at λ_{532}, while at λ_{785} this band is present only for SCC and papilloma (Figs. 2c, 2d). CH_2 oscillations are illustrated by peak at 1438 cm^{-1} [46], which broadens in all spectra of tumors at both laser excitation wavelengths. Its area decreases for BCC and SCC and increases for papilloma at λ_{532}, increases in BCC and stays unchanged in SCC and papilloma at λ_{785}. The similar decrease of the area under the curve was reported in earlier work [36]. The peak demonstrates a significant shift to the higher wavenumbers in the malignant skin spectra for both laser excitation wavelengths, with the variation being more pronounced for SCC and papilloma, which may be caused by stronger damage of the lipids' molecular structure.

Another band at 1416 cm^{-1} was attributed to molecular oscillations in ceramide III (Fig. 2, Table S2). Ceramides are also present in the cell membrane, so the observed band shift towards higher wavenumbers for all skin neoplasms at both excitation wavelengths may be due to disruption of the molecular structure of lipids in skin malignancies [28, 31]. Its intensity increases in BCC and SCC at λ_{532} and decreases for all tumors at λ_{785} according to the second derivative spectra (Fig. 2).

The band at 1459 cm^{-1} is attributed to proteins and lipids both [28, 31], and its area decreases in SCC and papilloma (more pronounced in SCC), and increases in BCC for both laser excitation wavelengths (Fig. 2, Table S2).

Interestingly, initially single band at 1744 cm^{-1} in spectra of normal skin, attributed to ester oscillations in lipids [47], was split into two weak bands at λ_{532} (Fig. 2, Table S2). Such trend was not observed for λ_{785}, where the band at 1745 cm^{-1} shifted to higher wavenumbers in SCC and to lower wavenumbers in papilloma, broadening in all spectra of tumors. This might be caused by the high noise level, making the changes insignificant.

3.1.4. Proteins. The band at 937 cm^{-1} was attributed to collagen [29, 39, 46], and in the malignant skin spectra it demonstrates broadening and area increase at λ_{532}, narrowing and area decrease—at λ_{785} (Fig. 2, Table S2). The band at 971 cm^{-1}, also attributed to proteins [39], in tumors' spectra splits into two bands, almost disappearing in papillomas at λ_{532}. At λ_{785} in malignant skin spectra only one of two bands is seen. Bands at 961 and 983 cm^{-1} illustrate molecular vibrations of α-helices and β-sheets in proteins, correspondingly. Such splitting may be caused by the possible changes in keratinocytes, arising from the atypical nuclei (enlarged, asymmetrical, hyperchromic) in SCC [48]. The secondary structure of histones mainly consists of α-helices, while fibrin mainly consists of β-sheets, therefore the observed increase in the 983 cm^{-1} band intensity is caused by fibrin, surrounding the cancer cells and forming a protective layer from the immune system cells. Such trend was observed earlier in a number of works [49–52].

The band at 1004 cm^{-1} corresponds to phenylalanine (Phe) vibrations [28, 34], and it narrows in the tumors' spectra at λ_{532} and broadens at λ_{785} (Fig. 2, Table S2). Supposedly, Phe is also present in spectra as bands at 1582 and 1605 cm^{-1} [53]. The 1582 cm^{-1} band width and area increase significantly SCC and papilloma (Fig. 2, Table S2), decreasing in BCC at λ_{532}, and vice versa—at λ_{785}. The band at 1605 cm^{-1} [54] narrows significantly in SCC and papilloma at λ_{532}, and broadens at λ_{785}. The corresponding area decreases in SCC spectra at λ_{532} and stays unchanged at λ_{785}; still, one must take into account the contribution of tyrosine and cytosine in the band intensity. The strong area increase of the band at 1605 cm^{-1} in tumors was reported earlier [55]. The band area in BCC and papilloma increases for both laser excitation wavelengths (Fig. 2, Table S2). The band at 1609–1615 cm^{-1} is related to tyrosine; in SCC it shifts to the lower wavenumbers at λ_{532}, and to higher wavenum-

bers in all malignant skin at λ_{785}. It becomes more pronounced in tumors at both laser excitation wavelengths, which may result to its narrowing. According to the second derivative spectra, its intensity increases in malignant skin spectra at λ_{532}, area decreasing at λ_{785}. The band at 1204 cm^{-1}, related to proteins, in the tumors' spectra shifts to higher wavenumbers at λ_{532}; its corresponding area increases for both laser excitation wavelengths (Fig. 2).

The band at 1537 cm^{-1} corresponds to amide II [56]. Its intensity at λ_{532} demonstrates a slight decrease in SCC, and it disappears completely in papilloma (Fig. 2); the band is not detected in spectra, acquired at λ_{785}.

Amide III (β-sheets) -related band in normal skin is located at 1264 cm^{-1}. According to literature, its transition to disordered state provides another band at 1245 cm^{-1} [10, 28], and such trend was observed for all malignant skin samples (Fig. 2, Table S2). The band at 1264 cm^{-1} in the spectra of tumors has a lower intensity and width, than in normal skin (Table S2). The band shift to higher wavenumbers was reported earlier [57] and was attributed to the arising destruction of the proteins' secondary structure. Another peak at 1252 cm^{-1} appears BCC for both laser excitation wavelengths, whereas in papilloma this peak is only seen at λ_{785}. This peak may also illustrate the disordered state of the proteins' secondary structure. The band at 1264 cm^{-1} was earlier observed only in healthy cells and was absent in malignant skin tumors [55]. In our work, the pronounced peak at 1264 cm^{-1} becomes weaker in BCC, SCC and papilloma, and the 1245 cm^{-1} peak area increases. Such variation in the proteins' secondary structure indicates the arising changes in the skin cells' structure in the tumor, such as an increase in fibrin content [55, 57].

Amide I band at 1654 cm^{-1} shifts to lower wavenumbers in BCC and SCC and to higher wavenumbers—in papilloms; its bandwidth in tumors increases for both laser excitation wavelengths. Such trend was reported earlier in a number of [28, 36]. The peak area decreases in BCC and increases in SCC and papilloma. The band intensity decrease in BCC was reported earlier [58]. Such changes may be attributed to the fact, that histones' secondary structure in normal skin mainly consists of α-helices, and their content in cancer cells is lowered, or the nucleic acids' structure is damaged [55]. Another amide I-related band at 1690 cm^{-1} is detected only at λ_{785}, and in SCC and papilloma its bandwidth and area increase.

C=C, N–H and C–N vibrations of amide II correspond to the band 1553 cm^{-1} [59], which demonstrates an increase in bandwidth and area in SCC and papilloma at λ_{532} (Fig. 2, Table S2). The band narrows in SCC and papilloma at λ_{785}. This peak may be also attributed to tryptophan, and its increase was reported earlier in BCC and SCC [60].

The band at 1513 cm^{-1} was attributed to carotenoids [32, 33]. Its intensity increases in spectra of papilloma and decreases in SCC, staying unchanged in BCC. Despite the fact, that some works report the higher content of carotenoids in BCC than in normal skin [39], there was no such trend in our work. Also, the carotenoids' content may vary depending on the individual patients' characteristics and their lifestyle (smoking, chronic fatigue, diseases etc.) [42].

Formation of BCC is often accompanied by the nucleus shape change to oval or elongated with condensed chromatin [58, 61]. The densification of the chromatin structure, which consists of DNA and proteins, leads to the corresponding Raman bands' narrowing. According to the second derivative spectra, the narrowing is observed in the bands at 1030, 1615, and 1655 cm^{-1}, which correspond to proteins and DNA (true for both used laser excitation wavelengths).

In BCC and SCC, mutations of protein p53 mainly consist of C → T and CC → TT transitions, and are triggered by ultraviolet (UV) radiation [62]. Such transition may lead to decrease in C concentration. Area of the band at 1260 cm^{-1}, which illustrates the C content, decreases in all spectra of tumors: BCC, SCC and papilloma. According to the literature [63], Raman bands, attributed to T, are located at 936 cm^{-1} (this band increases in BCC, SCC); 1063 cm^{-1} (increases in BCC and SCC); 1104, 1174, 1489, 1550 cm^{-1} (increase in SCC); 1232–1239, 1340 cm^{-1} (increase in all tumors).

4. CONCLUSIONS

In this work, we differentiated skin tumors (basal cell carcinoma, squamous cell carcinoma, papilloma) and healthy skin by analyzing the Raman bands' parameters based on the second derivative and the Lorentzian approximation of the spectra. It has been established that skin tumors can induce deformation of the secondary structure of proteins, resulting in a band at 972 cm^{-1} splitting into two peaks or shifting to lower wavenumbers. Another band, attributed to α-helices in proteins (1655 cm^{-1}), shows an increase in width and area in SCC and papilloma and a decrease in BCC. In addition, a band corresponding to the disordered state of amide III appears in tumors. Similar change in content of α-helices can be explained by disruption of their molecular structure in tumors. At the same time, in tumors the bands which illustrate the lipid content (1061, 1127, 1297, 1439, 1745 cm^{-1}), demonstrate broadening and/or area increase. Another feature associated with lipids is the splitting of the band at 1744 cm^{-1} into two peaks upon excitation at a wavelength of 532 nm and its significant broadening at 785 nm. The disruption of lipid structure, also

indicated in several bands as a "red" shift in wavenumbers, along with an increase in their content, is possibly associated with increased fluidity of the cell membrane.

The study of the spectra of papillomas is preliminary and may not be entirely objective due to the small sample size. The main goal of the work was to test the method of analyzing Raman spectra using the Lorentzian approximation. The results of using this method to analyze the spectra of skin tumors showed its promise for identifying characteristic biomarkers of malignant tumors and ongoing changes in cell structure, which can be the basis for differentiation in early diagnosis.

SUPPLEMENTARY INFORMATION

The online version contains supplementary material available at https://doi.org/10.1134/S0021364023604153.

FUNDING

The study was supported by the Russian Science Foundation, project no. 23-25-00249.

ETHICS APPROVAL AND CONSENT TO PARTICIPATE

All studies were conducted in accordance with the principles of biomedical ethics as outlined in the 1964 Declaration of Helsinki and its later amendments. They were also approved by the Interuniversity Ethics Committee of the Moscow State University of Medicine and Dentistry, protocol no. 3 dated March 3, 2023.

Each participant in the study provided a voluntary written informed consent after receiving an explanation of the potential risks and benefits, as well as the nature of the upcoming study.

CONFLICT OF INTEREST

The authors of this work declare that they have no conflicts of interest.

OPEN ACCESS

This article is licensed under a Creative Commons Attribution 4.0 International License, which permits use, sharing, adaptation, distribution and reproduction in any medium or format, as long as you give appropriate credit to the original author(s) and the source, provide a link to the Creative Commons license, and indicate if changes were made. The images or other third party material in this article are included in the article's Creative Commons license, unless indicated otherwise in a credit line to the material. If material is not included in the article's Creative Commons license and your intended use is not permitted by statutory regulation or exceeds the permitted use, you will need to obtain permission directly from the copyright holder. To view a copy of this license, visit http://creativecommons.org/licenses/by/4.0/

REFERENCES

1. V. V. Tuchin, *Handbook of Optical Biomedical Diagnostics,* 2nd ed. (SPIE Press, Bellingham, WA, 2016), p. 1410.
2. V. Tuchin, J. Popp, and V. Zakharov, *Multimodal Optical Diagnostics of Cancer* (Springer, Cham, Switzerland, 2020), p. 597. https://doi.org/10.1007/978-3-030-44594-2
3. V. P. Zakharov, K. V. Larin, S. V. Kozlov, A. A. Moryatov, I. A. Bratchenko, O. O. Myakinin, D. N. Artem'ev, and Yu. A. Khristoforova, Fiz. Voln. Prots. Radiotekh. Sist. **16** (3), 73 (2013).
4. S. V. Kozlov, V. Zakharov, A. A. Moryatov, I. A. Bratchenko, and D. N. Artem'ev, Izv. Samar. Nauch. Tsentra RAN **17**, 542 (2015).
5. I. A. Bratchenko, D. N. Artemyev, O. O. Myakinin, Y. A. Khristoforova, A. A. Moryatov, S. V. Kozlov, and V. P. Zakharov, J. Biomed. Opt. **22**, 027005 (2017).
6. I. A. Bratchenko, L. A. Bratchenko, A. A. Moryatov, Y. A. Khristoforova, D. N. Artemyev, O. O. Myakinin, A. E. Orlov, S. V. Kozlov, and V. P. Zakharov, Exp. Dermatol. **30**, 652 (2021).
7. A. N. Bashkatov, V. P. Zakharov, A. B. Bucharskaya, E. G. Borisova, Y. A. Khristoforova, E. A. Genina, and V. V. Tuchin, Opt. Diagn. Cancer **3**, 106 (2020).
8. R. Haydock, Ph.D. Thesis (Univ. Nottingham, Nottingham, UK, 2015).
9. A. Synytsya, M. Judexova, D. Hoskovec, M. Miskovicova, and L. Petruzelka, J. Raman Spectrosc. **45**, 903 (2014). https://doi.org/10.1002/jrs.4581
10. I. Matveeva, I. Bratchenko, Y. Khristoforova, L. Bratchenko, A. Moryatov, S. Kozlov, O. Kaganov, and V. Zakharov, Sensors **22**, 9588 (2022). https://doi.org/10.3390/s22249588
11. M. Larion, T. Dowdy, V. Ruiz-Rodado, M. W. Meyer, H. Song, W. Zhang, D. Davis, M. R. Gilbert, and A. Lita, Biosensors **9**, 5 (2019). https://doi.org/10.3390/bios9010005
12. A. N. Kuzmin, A. Pliss, A. Rzhevskii, A. Lita, and M. Larion, Biosensors **8**, 106 (2018). https://doi.org/10.3390/bios8040106
13. G. F. Silveira, D. M. Strottmann, L. de Borba, D. S. Mansur, N. I. T. Zanchin, and J. Bordignon, Clin. Exp. Immunol. **183**, 114 (2016). https://doi.org/10.1111/cei.12701
14. M. D. Keller, E. M. Kanter, and A. Mahadevan-Jansen, Spectroscopy **21** (11), 33 (2006).
15. M. A. Short, H. Lui, D. McLean, H. Zeng, A. Alajlan, and X. K. Chen, J. Biomed. Opt. **11**, 034004 (2006). https://doi.org/10.1117/1.2209549
16. E. Rimskaya, S. Shelygina, A. Timurzieva, I. Saraeva, E. Perevedentseva, N. Melnik, K. Kudrin, D. Reshetov, and S. Kudryashov, Int. J. Mol. Sci. **24**, 14748 (2023). https://doi.org/10.3390/ijms241914748

17. A. Cios, M. Ciepielak, L. Szymanski, A. Lewicka, S. Cierniak, W. Stankiewicz, M. Mendrycka, and S. Lewicki, Int. J. Mol. Sci. **22**, 2437 (2021). https://doi.org/10.3390/ijms22052437
18. I. Saraeva, D. Zayarny, E. Tolordava, A. Nastulyavichus, R. Khmelnitsky, D. Khmelenin, S. Shelygina, and S. Kudryashov, Chemosensors **11**, 361 (2023). https://doi.org/10.3390/chemosensors11070361
19. I. Saraeva, E. Tolordava, S. Sheligyna, A. Nastulyavichus, R. Khmelnitskii, N. Pokryshkin, D. Khmelenin, S. Kudryashov, A. Ionin, and A. Akhmatkhanov, Int. J. Mol. Sci. **24**, 5119 (2023). https://doi.org/10.3390/ijms24065119
20. X. Lu, Q. Liu, J. A. Benavides-Montano, A. V. Nicola, D. E. Aston, B. A. Rasco, and H. C. Aguilar, J. Virol. **87**, 3130 (2013). https://doi.org/10.1128/jvi.03220-12
21. A. O'Grady, A. C. Dennis, D. Denvir, J. J. McGarvey, and S. E. Bell, Anal. Chem. **73**, 2065 (2001).
22. M. N. Kinalwa, E. W. Blanch, and A. J. Doig, Anal. Chem. **82**, 6347 (2010).
23. C. A. Tellez Soto, L. P. Medeiros-Neto, L. dos Santos, A. B. Santos, I. Ferreira, P. Singh, R. Canevari, and A. A. Martin, J. Raman Spectrosc. **49**, 1165 (2018). https://doi.org/10.1002/jrs.5370
24. C. E. E. Grace, M. B. Mary, S. Vaidyanathan, and S. Srisudha, Spectrochim. Acta, Part A **270**, 120830 (2022).
25. L. Chrit, X. S. Hadjur, C. Morel, G. Sockalingum, G. Lebourdon, F. Leroy, and M. Manfait, J. Biomed. Opt. **10**, 044007 (2005).
26. C. A. Tellez-Soto, M. G. P. Silva, L. dos Santos, T. D. O. Mendes, P. Singh, S. A. Fortes, P. Favero, and A. A. Martin, Vibr. Spectrosc. **112**, 103196 (2021).
27. J. Zhao, H. Lui, D. I. McLean, and H. Zeng, Appl. Spectrosc. **61**, 1225 (2007).
28. X. Feng, A. J. Moy, H. T. Nguyen, J. Zhang, M. C. Fox, K. R. Sebastian, J. S. Reichenberg, M. K. Markey, and J. W. Tunnell, Biomed. Opt. Express **8**, 2835 (2017). https://doi.org/10.1364/BOE.8.002835
29. P. J. Caspers, G. W. Lucassen, R. Wolthuis, H. A. Bruining, and G. J. Puppels, Biospectroscopy **4** (4S), S31 (1998). https://doi.org/10.1002/(SICI)1520-6343(1998)4:5+<S31::AID-BSPY4>3.0.CO;2-M/
30. M. Gniadecka, P. A. Philipsen, S. Sigurdsson, O. F. Nielsen, D. H. Christensen, J. Hercogova, K. Rossen, H. K. Thomsen, and L. K. Hansen, J. Invest. Dermatol. **122**, 443 (2004). https://doi.org/10.1046/j.0022-202X.2004.22208.x
31. J. Anastassopoulou, M. Kyriakidou, E. Malesiou, M. Rallis, and T. Theophanides, Infrared Raman Spectrosc. Stud. Mol. Disord. Skin Cancer **33**, 567 (2019). https://doi.org/10.21873/invivo.11512
32. M. E. Darvin, W. Sterry, J. Lademann, and T. Vergou, Molecules **16**, 10491 (2011). https://doi.org/10.3390/molecules161210491
33. A. Morovati, M. A. Ansari, and V. V. Tuchin, J. Biophotonics **13**, e202000124 (2020). https://doi.org/10.1002/jbio.202000124
34. K. Maquelin, C. Kirschner, L. P. Choo-Smith, N. van der Braak, H. P. Endtz, D. Naumann, and G. J. Puppels, J. Microbiol. Methods **51**, 255 (2002). https://doi.org/10.1016/S0167-7012(02)00127-6
35. S. Bashir, H. Nawaz, M. I. Majeed, M. Mohsin, S. Abdullah, S. Ali, N. Rashid, M. Kashif, F. Batool, M. Abubakar, S. Ahmad, and A. Abdulraheem, Photodiagn. Photodyn. Ther. **34**, 102280 (2021). https://doi.org/10.1016/j.pdpdt.2021.102280
36. Y. Choi, J. W. Yoon, J. K. Hong, Y. Ryu, and S. H. Song, Commun. Phys. **3**, 1 (2020). https://doi.org/10.1038/s42005-020-00409-y
37. Y. Chen, J. Dai, X. Zhou, Y. Liu, W. Zhang, and G. Peng, PLoS One **9**, e93906 (2014). https://doi.org/10.1371/journal.pone.0093906
38. G. F. Silveira, D. M. Strottmann, L. de Borba, D. S. Mansur, N. I. T. Zanchin, J. Bordignon, and C. N. Duarte dos Santos, Clin. Exp. Immunol. **183**, 114 (2016). https://doi.org/10.1111/cei.12701
39. S. Tfaili, C. Gobinet, G. Josse, J. F. Angiboust, M. Manfait, and O. Piot, Analyst **137**, 3673 (2012). https://doi.org/10.1039/C2AN16292J
40. Y. Li, Z. N. Wen, L. J. Li, M. L. Li, N. Gao, and Y. Z. Guo, J. Raman Spectrosc. **41**, 142 (2010). https://doi.org/10.1002/jrs.2421
41. S. Rauniyar, K. Pansare, A. Sharda, S. R. Singh, P. Saha, M. K. Chilakapati, and S. Gupta, ACS Omega **8**, 5522 (2023). https://doi.org/10.1021/acsomega.2c06787
42. N. Kourkoumelis, I. Balatsoukas, V. Moulia, A. Elka, G. Gaitanis, and I. D. Bassukas, Int. J. Mol. Sci. **16**, 14554 (2015). https://doi.org/10.3390/ijms160714554
43. M. Kashif, M. I. Majeed, M. A. Hanif, and A. ur Rehman, Spectrochim. Acta, Part A **242**, 118729 (2020). https://doi.org/10.1016/j.saa.2020.118729
44. X. Y. Liu, P. Zhang, L. Su, L. M. Wang, X. D. Wei, H. Q. Wang, and T. F. Lin, J. Nanosci. Nanotechnol. **18**, 6776 (2018). https://doi.org/10.1166/jnn.2018.15510
45. R. Vyumvuhore, A. Tfayli, H. Duplan, A. Delalleau, M. Manfait, and A. Baillet-Guffroy, Analyst **138**, 4103 (2013). https://doi.org/10.1039/C3AN00716B
46. D. Lunter, V. Klang, D. Kocsis, Z. Varga-Medveczky, S. Berko, and F. Erdo, Exp. Dermatol. **31**, 1311 (2022). https://doi.org/10.1111/exd.14645
47. P. Rekha, P. Aruna, E. Brindha, D. Koteeswaran, M. Baludavid, and S. Ganesan, J. Raman Spectrosc. **47**, 763 (2016). https://doi.org/10.1002/jrs.4897
48. V. Ratushny, M. D. Gober, R. Hick, T. W. Ridky, and J. T. Seykora, J. Clin. Invest. **122**, 464 (2012). https://doi.org/10.1172/JCI57415
49. R. Vilar, R. J. Fish, and A. Casini, Haematologica **105**, 284 (2020). https://doi.org/10.3324/haematol.2019.236901
50. A. Collen, S. M. Smorenburg, E. Peters, F. Lupu, P. Koolwijk, C. van Noorden, and V. W. van Hinsbergh, Cancer Res. **60**, 6196 (2000).

51. H. F. Dvorak, D. R. Senger, and A. M. Dvorak, Cancer Metastasis Rev. **2**, 41 (1983). https://doi.org/10.1007/BF00046905

52. T. M. Niers, L. W. Bruggemann, C. P. Klerk, F. J. M. Muller, T. Buckle, P. H. Reitsma, D. J. Richel, C. A. Spek, O. van Tellingen, and C. J. F. van Noorden, Clin. Exp. Metast. **26**, 171 (2009). https://doi.org/10.1007/s10585-008-9227-6

53. Z. Q. Wen, X. Cao, and A. Vance, J. Pharm. Sci. **97**, 2228 (2008). https://doi.org/10.1002/jps.21191

54. H. Jayan, H. Pu, and D. W. Sun, Spectrochim. Acta, Part A **276**, 121217 (2022). https://doi.org/10.1016/j.saa.2022.121217

55. Y. Chen, J. Dai, X. Zhou, Y. Liu, W. Zhang, and G. Peng, PLoS One **9**, e93906 (2014). https://doi.org/10.1371/journal.pone.0093906

56. A. Falamaş, S. A. Cinta-Pinzaru, C. Dehelean, C. H. Krafft, and J. Popp, Rom. J. Biophys **20** (1), 1 (2010).

57. N. Kourkoumelis, I. Balatsoukas, V. Moulia, G. Gaitanis, and I. D. Bassukas, Int. J. Mol. Sci. **16**, 14554 (2015). https://doi.org/10.3390/ijms160714554

58. M. Gniadecka, H. C. Wulf, N. Nymark Mortensen, O. Faurskov Nielsen, and D. H. Christensen, J. Raman Spectrosc. **28**, 125 (1997). https://doi.org/10.1002/(SICI)1097-4555(199702)28:2/3<125::AID-JRS65>3.0.CO;2-%23

59. D. Predoi, S. L. Iconaru, M. Albu, C. C. Petre, and G. Jiga, Polym. Eng. Sci. **57**, 537 (2017). https://doi.org/10.1002/pen.24553

60. C. A. Lieber, S. K. Majumder, D. Billheimer, D. L. Ellis, and A. Mahadevan-Jansen, J. Biomed. Opt. **13**, 024013 (2008). https://doi.org/10.1117/1.2899155

61. E. B. Souto, R. da Ana, V. Vieira, J. F. Fangueiro, J. Dias-Ferreira, A. Cano, A. Zielinska, A. M. Silva, R. Staszewski, and J. Karczewski, Neoplasia **30**, 100810 (2022). https://doi.org/10.1016/j.neo.2022.100810

62. S. Bolshakov, C. M. Walker, S. S. Strom, M. S. Selvan, G. L. Clayman, A. El-Naggar, S. M. Lippman, M. L. Kripke, and H. N. Ananthaswamy, Clin. Cancer Res. **9**, 228 (2003).

63. N. Leopold, S. Cinta-Pinzaru, M. Baia, E. Antonescu, O. Cozar, W. Kiefer, and J. Popp, Vibr. Spectrosc. **39**, 169 (2005). https://doi.org/10.1016/j.vibspec.2005.02.019

Translated by the authors

Publisher's Note. Pleiades Publishing remains neutral with regard to jurisdictional claims in published maps and institutional affiliations.